

1 **Isotopic composition of nitrate and particulate organic matter in a**  
2 **pristine dam-reservoir of western India: Implications for**  
3 **biogeochemical processes**

4 Pratrupa Bardhan, S.W.A. Naqvi, Supriya G. Karapurkar, Damodar M. Shenoy, Siby Kurian,  
5 Hema Naik.

6 CSIR-National Institute of Oceanography, Dona Paula, Goa:403004, India.

7 *Correspondence to:* P.Bardhan ([pratirupabardhan@gmail.com](mailto:pratirupabardhan@gmail.com))

8

9

10

11

12

13

14

15

16

17

18

19

20

21

22

23

24

25 **Abstract:**

26  
27 Isotopic composition of nitrate ( $\delta^{15}\text{N}$  and  $\delta^{18}\text{O}$ ) and particulate organic matter (POM) ( $\delta^{15}\text{N}$   
28 and  $\delta^{13}\text{C}$ ) were measured in Tillari Reservoir, located at the foothills of the Western Ghats,  
29 Maharashtra, western India. The reservoir that is stratified during spring-summer and autumn  
30 seasons but gets vertically mixed during the Southwest Monsoon (SWM) and winter is  
31 characterized by diverse redox nitrogen transformations in space and time. The  $\delta^{15}\text{N}$  and  $\delta^{18}\text{O}$   
32 values of nitrate were low ( $\delta^{15}\text{N} = 2\text{-}10\text{‰}$ ,  $\delta^{18}\text{O} = 5\text{-}8\text{‰}$ ) during normoxic conditions but  
33 increased gradually (highest  $\delta^{15}\text{N}=27\text{‰}$ ,  $\delta^{18}\text{O}=29\text{‰}$ ) when anoxic conditions facilitated  
34 denitrification in the hypolimnion during spring-early summer. Once nitrate was fully utilized  
35 and sulphidic conditions set in,  $\text{NH}_4^+$  became the dominant inorganic N species, with  $\delta^{15}\text{N}$   
36 ranging from 1.3 to 2.6‰. Low  $\delta^{15}\text{N}$  ( $\sim -5\text{‰}$ ) and  $\delta^{13}\text{C}$  ( $-37\text{‰}$  to  $-32\text{‰}$ ) of POM co-  
37 occurring with high  $\text{NH}_4^+$  and  $\text{CH}_4$  in sulphidic bottom waters were probably the  
38 consequence of microbial chemosynthesis. Assimilation of nitrate in the epilimnion was the  
39 major controlling process on the N-isotopic composition of POM ( $\delta^{15}\text{N} = 2 - 6 \text{‰}$ ). Episodic  
40 low  $\delta^{15}\text{N}$  values of POM ( $-2$  to  $0\text{‰}$ ) during early summer coinciding with the absence of  
41 nitrate might arise from N-fixation, although further work is required to confirm the  
42 hypothesis.  $\delta^{13}\text{C}$ -POM in the photic zone ranged between  $-29\text{‰}$  and  $-27\text{‰}$  for most parts of  
43 the year. The periods of mixing were characterized by uniform  $\delta^{15}\text{N}\text{-NO}_3^-$  and  $\delta^{18}\text{O}\text{-NO}_3^-$  at  
44 all depths. Higher POM ( particulate organic carbon (POC) as well as particulate organic  
45 nitrogen (PON)) contents and C/N values with lower  $\delta^{13}\text{C}$ -POM during the SWM point to  
46 allochthonous inputs. Overall, this study, the first of its kind in the Indian subcontinent,  
47 provides an insight into biogeochemistry of Indian reservoirs, using stable carbon and  
48 nitrogen isotopes as a tool, where the monsoons play an important role in controlling vertical  
49 mixing and dynamics of carbon and nutrients.

50

## 51 **1.Introduction:**

52 Nitrogen is an essential macronutrient the availability of which often limits primary  
53 production in aquatic ecosystems. It is a polyvalent element that undergoes redox  
54 transformation between the terminal oxidation states of +5 and -3. These transformations  
55 involve isotopic fractionation to varying degrees, and so natural abundance of stable isotopes  
56 ( $^{15}\text{N}$  and  $^{14}\text{N}$ ) in various N species provides useful insight into nitrogen cycling besides its  
57 sources/sinks in the oceanic (Altabet, 1988; Sigman et al., 2005), coastal (Thunell et al.,  
58 2004; Hu et al., 2015) and estuarine (Cifuentes et al, 1988; Savoye et al., 2012) water-bodies  
59 and sediments. Studies have also been undertaken in freshwater systems like lakes (Pang and  
60 Nriagu, 1977; Chen et al., 2014) and reservoirs (Chen and Jia, 2009; Junet et al., 2009). Some  
61 of the best studied freshwater ecosystems in this regard are Lake Lugano at the Swiss-Italian  
62 border, Lake Kinneret in Israel and Lake Superior in the USA.

63 In the eutrophic Lake Lugano, the highly depleted  $\delta^{13}\text{C}$  and  $\delta^{15}\text{N}$  of the near-bottom POM  
64 established the active presence of methanotrophic bacteria during suboxic conditions  
65 (Lehmann et al., 2004). Seasonal changes in nitrogen species were reflected in the isotopic  
66 composition of particulate organic matter (POM) and dissolved inorganic nitrogen (DIN)  
67 compounds in Lake Kinneret (Hadas et al., 2009). Various processes like nitrification,  
68 denitrification and  $\text{N}_2$ -fixation were identified with the help of the N isotopes. In Lake  
69 Superior, based on nitrate isotopic studies it was possible to identify the increasing inputs of  
70 reduced N to the lake and its subsequent nitrification to be the cause behind a century-long  
71 increase in the nitrate inventory of the lake, ruling out atmospheric deposition as the other  
72 probable cause (Finlay et al., 2007).

73 There are a large number of natural freshwater lakes as well as man-made reservoirs in India.  
74 In fact, India has the third-highest number of dams (around 4300) in the world, after China  
75 and USA. However, these systems have not been well investigated for biogeochemical

76 cycling.. In the very first study of its kind, Narvenkar et al. (2013) sampled eight dam-  
77 reservoirs spread across India and observed strong thermal stratification during summer in all  
78 reservoirs. Six of these reservoirs were found to experience varying degrees of oxygen  
79 depletion in the hypolimnia, ranging from hypoxia to complete anoxia, in spring-summer.  
80 Anoxia has been found to greatly affect the distribution of nitrogen species in these systems.  
81 In order to gain insights into biogeochemical cycling in these poorly investigated water  
82 bodies, we selected the Tillari Reservoir for detailed studies. These included measurements of  
83 natural abundance of nitrogen and oxygen isotopes in nitrate, and nitrogen and carbon  
84 isotopes in POM. These data, first of their kind generated from any Indian freshwater body,  
85 facilitate an understanding of biogeochemical processes (especially involving nitrogen) that  
86 should be typical of any relatively pristine, tropical, monsoon-affected freshwater body.

87

## 88 **2.Methods:**

### 89 **2.1 Site Description:**

90 The Tillari Reservoir is situated in the Dodamarg *taluka* in the Sindhudurg district of  
91 Maharashtra (15°76'N, 74°12'E, Fig. 1). Created by damming the Tillari River, the reservoir  
92 has a maximum depth of ~50 m and a storage capacity of  $0.45 \times 10^9 \text{ m}^3$  (Kurian et al. 2012).  
93 The reservoir is located close to the foothills of the Western Ghats, with the drainage basin  
94 having evergreen forests (C3 plant type) as well as grasslands (C3 or C4 plant types)  
95 (Sukumar et al., 1995). The drainage basin of Tillari has low population density, and so the  
96 river water is not much impacted by human activities such as municipal and industrial  
97 discharges, and agriculture. This is reflected by high water quality (Shenoy et al., manuscript  
98 in preparation). The region receives rainfall averaging around 3000 mm annually, almost  
99 entirely between June and September. The evaporation rate in Tillari Reservoir is not known,  
100 but for other Indian reservoirs the evaporative loss is reported to average around 0.2 m

101 (Subramanya, 2013) per month. Water from Tillari Reservoir is mainly used for irrigation.  
102 Some watershed characteristics of the Tillari Reservoir have been listed in Supplementary  
103 Table 1.

104 The Tillari Reservoir is a dimictic water body. Relatively low air temperatures and cool  
105 winds descending from the Western Ghats, located immediately to the east of the reservoir,  
106 result in convective mixing and well oxygenated conditions in winter. The water column gets  
107 thermally stratified in spring and remains so until the strong SWM winds and supply of  
108 relatively cold water homogenize the water column again. The water column gets stratified  
109 after the SWM. Stratification during spring-summer leads to anoxic condition that is most  
110 intense (sulphidic in most years) just before the onset of mixing in June-July. A previous  
111 study (Kurian et al, 2012) showed that the occurrence of sulphidic conditions within the  
112 euphotic zone supports anoxygenic photosynthesis by brown sulphur bacteria in this  
113 reservoir. Methane has been found to accumulate in high concentrations below the  
114 thermocline during this period; however, its emissions to the atmosphere are not very high  
115 (Narvenkar et al., 2013). Direct human impacts on nutrient inventory of the reservoir are  
116 relatively minor, as the basin is located amidst thick forests with low human population  
117 density and minimum agricultural activities.

## 118 **2.2 Sampling and field measurements:**

119 Sampling was conducted at one station located at the deepest part of the reservoir. Water  
120 samples from pre-fixed depths were collected with 5-litre Niskin samplers attached to nylon  
121 ropes and equipped with reversing thermometers to measure temperature. Subsamples for  
122 dissolved oxygen (DO) and hydrogen sulfide (H<sub>2</sub>S) were collected carefully avoiding air  
123 exchange. Subsamples for nutrients (nitrate and ammonium) were collected in clean 60-ml  
124 HDPE bottles and frozen immediately. Subsamples for stable isotopic analyses were

125 collected in 5-litre acid-cleaned plastic carboys and transported to the laboratory within 3-4  
126 hours.

127

### 128 **2.3 Laboratory analyses:**

129

130 Dissolved O<sub>2</sub> was estimated by the Winkler method (Grasshoff et al., 1983) with a precision  
131 of <1 μM. NO<sub>3</sub><sup>-</sup> and NH<sub>4</sub><sup>+</sup> were measured using a SKALAR segmented flow analyzer  
132 following standard procedures (Grasshoff et al., 1983) with a precision of <0.1 μM.

133 Dissolved H<sub>2</sub>S concentration was determined colorimetrically (Cline, 1969).

134

### 135 **2.4 Isotopic analyses :**

136

137 Sampling for isotopic analyses of POM commenced in March 2010 and continued on a  
138 monthly basis till 2012. From 2012 to 2015 samples were collected on a seasonal basis.

139 Samples for nitrate isotopic measurements were collected from 2011. The facility for nitrate  
140 isotope analysis was created in 2014 and samples from 2014 and 2015 were analysed  
141 immediately for natural abundance of N and O isotopes. Samples from 2011 and 2012 were  
142 also analysed on a selective basis. Samples (upto 3l) for isotopic analyses of POM and DIN  
143 (dissolved inorganic nitrogen i.e. NO<sub>3</sub><sup>-</sup> and NH<sub>4</sub><sup>+</sup>) were filtered through precombusted (450°  
144 C for 4 hours) 47mm GF/F filters (pore size = 0.7 μm). The filtrate was used for DIN isotopic  
145 measurements and the filter papers were placed in petriplates and frozen immediately.

146

#### 147 **2.4.1 Analyses of δ<sup>15</sup>N and δ<sup>18</sup>O of NO<sub>3</sub><sup>-</sup>:**

148 Samples for isotopic analysis of nitrate were preserved in two ways. While samples collected  
149 in 2011 and 2012 were acidified with HCl to pH 2.5, those taken in 2014 and 2015 were  
150 frozen immediately and analysed within a week. Prior to the isotopic analyses, nitrate and  
151 nitrite concentrations were measured colorimetrically. Isotopic analyses of nitrogen and  
152 oxygen in NO<sub>3</sub><sup>-</sup> were carried out following the “chemical method” (McIlvin and Altabet,

153 2005) involving reduction of  $\text{NO}_3^-$  to  $\text{NO}_2^-$  by cadmium and further reduction to  $\text{N}_2\text{O}$  by  
154 sodium azide in an acetic acid buffer. The resulting  $\text{N}_2\text{O}$  gas in the headspace was purged  
155 into a GasBench II (Thermo Finnigan) and analysed in a Delta V isotope ratio mass  
156 spectrometer.

157 Nitrite concentration was insignificant in most of the samples; sulphamic acid was added in a  
158 few samples that contained nitrite in concentrations exceeding  $0.1 \mu\text{M}$ . Working standards  
159 were prepared in low-nutrient surface seawater (LNSW) collected from the Arabian Sea.  
160 Calibration was done using international nitrate isotope standards USGS-32, USGS-34 and  
161 USGS-35. For further quality assurance, an internal potassium nitrate standard (spanning the  
162 range of nitrate concentration in the samples) was run with each batch of samples.  
163 Magnesium oxide ( $\text{MgO}$ , Fisher; precombusted for 4 hours at  $450^\circ\text{C}$ ) was added to each  
164 sample to raise the pH close to 9 which was followed by addition of cadmium. We used  
165 cadmium powder (Alfa Aesar,  $-325$  mesh, 99.5%) instead of spongy cadmium as mentioned  
166 in McIlvin and Altabet (2005). Each vial was wrapped in aluminium foil and placed on a  
167 horizontal shaker at low speed for 17 hours. After the stipulated time, samples were removed  
168 from the shaker, centrifuged and decanted into clean vials. The nitrite concentrations in the  
169 decanted samples were measured to check the extent of reduction.

170 Sodium azide (2M solution) and 20% acetic acid were mixed in 1:1 proportion (by volume)  
171 to yield the azide-acetic acid buffer (A-AA buffer) solution. In 20 ml crimp vials, samples  
172 and standards were diluted with LNSW for a final concentration of 20 nmoles and a final  
173 volume of 15 ml. Two international nitrite standards (N23 and N20) were added in this step  
174 to check the efficiency of  $\text{N}_2\text{O}$  production by the buffer. After addition of the A-AA buffer,  
175 the vials were allowed to stand for 1 hour and then the reaction was stopped by adding 0.5ml  
176 of 10M NaOH.

177 The “chemical” method yielded a very low blank ( $\sim 0.5 \mu\text{M}$ ) and worked well for the low  
178 concentration samples. The international standards were run before and after each batch of  
179 samples, while the internal nitrate standards were run after every 5 samples. Analytical  
180 precision (one standard deviation) was better than 0.3‰ for  $\delta^{15}\text{N}$  and better than 0.7‰ for  
181  $\delta^{18}\text{O}$ . Results are expressed in  $\delta$  notation ( $\delta^{15}\text{N}$  and  $\delta^{18}\text{O}$ ), as per mil (‰) deviation from  
182 atmospheric nitrogen and Vienna Standard Mean Ocean Water (VSMOW), respectively.

#### 183 **2.4.2 Analyses of $\delta^{15}\text{N}$ of $\text{NH}_4^+$ :**

184 Samples for measurements of  $\delta^{15}\text{N}$ -  $\text{NH}_4^+$  was collected during May 2012 from the anaerobic  
185 hypolimnetic waters. The  $\delta^{15}\text{N}$  of  $\text{NH}_4^+$  was measured by the “ammonia diffusion” method  
186 (Holmes et al., 1998). Briefly, 500 ml of sample was collected in duplicates to which 1.5g of  
187 MgO was added to elevate the pH. The diffused  $\text{NH}_4^+$  was trapped onto acidified glass-fiber  
188 filter sealed between two porous Teflon membranes. The sample bottles were kept in an  
189 incubator-shaker (20°C, 80 rpm) for two weeks for complete diffusion of  $\text{NH}_4^+$ . After two  
190 weeks, the GF filters were removed from each sample, dried in a  $\text{NH}_4^+$ -free environment,  
191 packed into tin cups and immediately analysed using CF-EA-IRMS. Results were corrected  
192 for blank, percent recovery and fractionation. Analytical precision was better than 0.6‰.

#### 193 **2.4.3 Analyses of $\delta^{13}\text{C}$ and $\delta^{15}\text{N}$ of POM and surface sediment:**

194 The analyses of  $\delta^{13}\text{C}$  and  $\delta^{15}\text{N}$  of POM were usually conducted within 1-2 months of  
195 collection. The frozen filters were acid-fumed with 36% HCl to eliminate carbonates and air  
196 dried in a clean laminar flow. Two aliquots (each of 12 mm diameter) were sub-sectioned  
197 from each filter and packed into tin cups for analysis. Detailed methodology is given in Maya  
198 et al. (2011). The  $\delta^{13}\text{C}$  and  $\delta^{15}\text{N}$  of POM along with particulate C and N contents were  
199 analyzed in the same sample using a stable isotope ratio mass spectrometer (Thermo Finnigan  
200 Delta V) connected to an elemental analyser (EURO3000 Eurovector). Results are expressed  
201 as per mil (‰) deviation with respect to PDB (Pee Dee Belemnite) for  $\delta^{13}\text{C}$  and atmospheric



202 nitrogen for  $\delta^{15}\text{N}$ . Analytical precision was better than  $\pm 0.2\%$  as determined from repeated  
203 measurements (after every 5 samples) of a working standard,  $\epsilon$ -Amino-n-Caproic Acid  
204 (ACA) having  $\delta^{13}\text{C} = -25.3\%$  and  $\delta^{15}\text{N} = 4.6\%$ , and a laboratory sediment standard having  
205  $\delta^{13}\text{C} = -21\%$  and  $\delta^{15}\text{N} = 7.5\%$ .

206 Surface sediment collected from the reservoir during the May 2012 field trip was analysed on  
207 only one occasion to investigate its role as an ammonium source. The freeze-dried,  
208 homogenized sample was analyzed following similar protocol.

209

### 210 **3. Results**

#### 211 **3.1 Water column observations**

212 Based on the vertical temperature distribution it appears that the reservoir gets vertically  
213 mixed through convective overturning in winter (December to February, with the exact  
214 duration of mixing depending upon meteorological conditions prevailing in a given year). In  
215 spring stratification sets in and is the most intense from April to June/July (with a surface-to-  
216 bottom temperature difference of  $7-8^\circ\text{C}$ ). The water column is again homogenized following  
217 SWM induced mixing and flow of relatively cold water, followed by weaker stratification in  
218 autumn/early winter. A detailed discussion on the physico-chemical parameters is provided in  
219 Shenoy et al. (manuscript under preparation).

220 The epilimnion was always oxic. During the stratification periods, the DO concentrations  
221 dropped rapidly within the thermocline. The water column became well-oxygenated  
222 following the onset of the southwest monsoon.  $\text{H}_2\text{S}$  was detected below 20 m during the  
223 period of intense stratification (Kurian et al., 2012), with the highest concentration recorded  
224 being  $9.88\ \mu\text{M}$ . The occurrence of  $\text{H}_2\text{S}$  was accompanied by the appearance of  $\text{CH}_4$  and  
225  $\text{NH}_4^+$ . Upto  $160\ \mu\text{M}$  of  $\text{CH}_4$  and  $30\ \mu\text{M}$  of  $\text{NH}_4^+$  were observed in the anoxic bottom waters  
226 during peak summer (Narvenkar et al., 2013).

227 A thorough analysis of nutrient dynamics in Tillari Reservoir is provided by Naik et al.  
228 (manuscript under preparation). Here we provide a brief description of nitrate profiles during  
229 the study period. Surface water nitrate concentrations were typically low throughout the year  
230 ranging from below detection limit to 0.7  $\mu\text{M}$ . However, the surface nitrate concentrations  
231 were as high as  $\sim 10 \mu\text{M}$  (Fig. 3a) during the SW Monsoon. Nitrate concentrations gradually  
232 increased below the epilimnion during the period of weak stratification. However, with the  
233 depletion of DO, nitrate concentrations in the hypolimnion decreased from 3.6  $\mu\text{M}$  (at 20m)  
234 to 0.3  $\mu\text{M}$  (at 35m), indicating N-loss. Reoxygenation of hypolimnion during the SW  
235 monsoon was accompanied by increase in nitrate concentrations (5-10  $\mu\text{M}$ ).

### 236 **3.2 Isotopic composition of nitrate and ammonium**

237 Large variations in the isotopic composition of nitrate and ammonium were observed in space  
238 and time. Isotopic composition of nitrate in the epilimnion could not be measured on several  
239 occasions due to low concentrations. However, when the measurements could be made it was  
240 observed that the  $\delta^{15}\text{N}$  and  $\delta^{18}\text{O}$  values of epilimnetic (0-10 m)  $\text{NO}_3^-$  were high ( $\delta^{15}\text{N} = 8$ -  
241  $25\text{‰}$ ,  $\delta^{18}\text{O} = 24$ - $29\text{‰}$ ) (Fig 3b) during the summer stratification presumably due to  
242 autotrophic assimilation whereas relatively lower values ( $\delta^{15}\text{N} = 5$ - $8\text{‰}$ ,  $\delta^{18}\text{O} = 12$ - $15\text{‰}$ )  
243 were observed during the monsoon mixing events. Increasing  $\delta^{15}\text{N}$  and  $\delta^{18}\text{O}$  of  $\text{NO}_3^-$ ,  
244 coupled to decreasing  $[\text{NO}_3^-]$ , were also observed in the suboxic hypolimnion during April  
245 and May, when the water column was strongly stratified. The highest  $\delta^{15}\text{N}$  values observed  
246 were  $27.7\text{‰}$  (in 2014) and  $22.4\text{‰}$  (in 2012) while the corresponding highest  $\delta^{18}\text{O}$  values  
247 were  $29.5\text{‰}$  and  $28.8\text{‰}$ , respectively.

248 The water column remains weakly stratified for a large part of the year, usually from October  
249 to March. A trend of increasing concentrations of isotopically light ( $\delta^{15}\text{N} = 2$ - $8\text{‰}$  and  $\delta^{18}\text{O} =$   
250  $5$ - $8\text{‰}$ ) nitrate was observed in the hypolimnion along with gradually decreasing levels of

251 oxygen and ammonium implying the occurrence of nitrification. As the stratification  
252 intensified, this phenomenon was restricted only to the metalimnion. After nitrate was  
253 exhausted, high ammonium build up was observed in the bottom waters. In May 2012,  $\text{NH}_4^+$   
254 concentrations increased from 0.6  $\mu\text{M}$  at 20m to nearly 12  $\mu\text{M}$  at 40m with a corresponding  
255 decrease in  $\delta^{15}\text{N-NH}_4^+$  from 2.6‰ at 20m to 1.3‰ at 40m (Fig. 5a).

256 Elevated nitrate concentrations occur throughout the water column during the SW monsoon.  
257 The  $\delta^{15}\text{N}$  and  $\delta^{18}\text{O}$  of  $\text{NO}_3^-$  showed little vertical variations at this time. However,  
258 interannual variability was seen in the  $\delta^{15}\text{N}$  of nitrate ( $3.94 \pm 2.4\%$  in 2011,  $11.38 \pm 1.6\%$  in  
259 2014, and  $5.47 \pm 1.8\%$  in 2015), the cause of which will be examined. By contrast, the  $\delta^{18}\text{O-}$   
260  $\text{NO}_3^-$  values were relatively less variable ( $13.01 \pm 4.8\%$  in 2011,  $15.41 \pm 2.3\%$  in 2014, and  
261  $12.46 \pm 4.9\%$  in 2015).

### 262 **3.3 Isotopic and elemental composition of suspended particulate organic** 263 **matter**

264 The suspended particulate organic matter in the Tillari Reservoir showed distinct seasonal  
265 and depth-wise variations in its isotopic and elemental compositions (Fig. 2). Primary  
266 productivity in the epilimnion led to higher  $\delta^{15}\text{N}$  (2‰ to 6‰) and  $\delta^{13}\text{C}$  ( $-28\%$  to  $-26\%$ ) in  
267 POM and higher POC (35-60  $\mu\text{M}$ ) and PON (4-6  $\mu\text{M}$ ) contents as compared to the bottom  
268 water. The molar C/N ratios in the surface waters ranged between 7 and 10. Depleted  $\delta^{15}\text{N}$   
269 ( $\sim -1.4\%$ ) in the epilimnion was observed during the early stratification period (February and  
270 March). As the stratification intensified, the  $\delta^{15}\text{N}$  and  $\delta^{13}\text{C}$  of the epilimnetic POM became  
271 heavier, presumably reflecting a gradual enrichment of heavier isotopes in the dissolved  
272 inorganic N and C pools. Both  $\delta^{15}\text{N}$  and  $\delta^{13}\text{C}$  decreased with depth with the lowest values  
273 occurring in the anoxic bottom water during peak stratification period. The C/N values in  
274 these waters were in the range of 4-7. In terms of seasonal variability,  $\delta^{13}\text{C}$  values of POM

275 were lower during monsoon mixing and became more enriched as the stratification  
276 intensified. The  $\delta^{15}\text{N}$  values, however, did not depict any distinct seasonal pattern. High POC  
277 (upto 80  $\mu\text{M}$ ) and PON (upto 9  $\mu\text{M}$ ) along with high C/N (>10) were recorded during the  
278 monsoon season apparently reflecting allochthonous inputs.

## 279 **4. Discussion:**

### 280 **4.1 Epilimnetic processes:**

281 Nitrate concentrations in surface waters of the Tillari Reservoir varied from below detection  
282 limit during the premonsoon period to 10.7  $\mu\text{M}$  during the SW monsoon. The  $\delta^{18}\text{O}$  and  $\delta^{15}\text{N}$   
283 values of nitrate in the epilimnion were high, a signature of assimilation: phytoplankton  
284 prefer nitrate containing  $^{14}\text{N}$  and  $^{16}\text{O}$  leaving residual nitrate enriched with  $\delta^{15}\text{N}$  and  $\delta^{18}\text{O}$   
285 (Casciotti et al., 2002). We examined the slopes of the  $\delta^{18}\text{O}$  vs.  $\delta^{15}\text{N}$  regression in the surface  
286 water. While a 1:1 line would represent assimilation of epilimnetic nitrate, a steeper slope  
287 would imply assimilation along with the regeneration of nitrate via nitrification (Wankel et  
288 al., 2007). We observed a nearly 1:1 trend for most of the surface water samples during the  
289 summer stratification implying that assimilation exerts the major control on surface  $\text{NO}_3^-$   
290 isotopic composition (Supplementary Fig. 1).

291 The isotopic composition of the DIN source exerts the key control on the  $\delta^{15}\text{N}$  of POM  
292 (Altabet, 2006). The epilimnetic POM in the Tillari Reservoir is expected to have  $\delta^{15}\text{N}$  less  
293 than or equal to the  $\delta^{15}\text{N}\text{-NO}_3^-$ . Indeed, the  $\delta^{15}\text{N}\text{-POM}$  was always lower than the  $\delta^{15}\text{N}$  of the  
294 source nitrate (Fig. 3b). The range of  $\delta^{13}\text{C}$  values of surface-water POM (-32 to -26‰) was  
295 typical of lacustrine autochthonous organic matter (-42 to -24‰, Kendall et al., 2001 and  
296 references therein). As the summer progressed, productivity increased resulting in increased  
297  $\text{CO}_2$  uptake and elevated  $\delta^{13}\text{C}\text{-POM}$ . During photosynthesis, phytoplankton preferentially

298 uptake  $^{12}\text{C}$  leaving the DIC (dissolved inorganic carbon) pool enriched in  $^{13}\text{C}$ . However,  
299 when dissolved C is scarce and/or growth rate is high, the phytoplankton would consume the  
300 available DIC with reduced or no isotopic discrimination. As the summer progressed at the  
301 study location, increased water temperature and low dissolved inorganic nutrient and DIC  
302 concentrations would cause the phytoplankton to express reduced isotopic discrimination.  
303 This would result in enriched  $\delta^{13}\text{C}$  of POM. Similar enrichment of  $\delta^{13}\text{C}$ -POM during periods  
304 of high productivity have also been observed in other lakes, for e.g., Lake Lugano (Lehmann  
305 et al., 2004) and Lake Wauberg (Gu et al., 2006).

306 In March, when nitrate was close to detection limit, surface  $\delta^{15}\text{N}$ -POM was  $-1.4\%$ . The  
307 POM resulting from nitrogen fixation by cyanobacteria usually has a  $\delta^{15}\text{N}$  of 0 to  $-2\%$   
308 (Carpenter et al., 1997). Zeaxanthin, marker pigment of cyanobacteria, was present in  
309 significant concentrations ( $305.1 \pm 21 \text{ ng l}^{-1}$ ) within the epilimnion, whereas Chl-*a*  
310 concentration was  $\sim 1.7 \mu\text{g l}^{-1}$  (S. Kurian, unpublished data). However, measurements of  
311 nitrogen fixation rates in the Tillari Reservoir have yielded very low values during summer  
312 (unpublished data). Alternatively, the lower  $\delta^{15}\text{N}$  values may also result from isotopically  
313 light nitrate that is produced in the hypolimnion and diffuses upward into surface waters.  
314 Another possible source of isotopically lighter N could be atmospheric deposition, although  
315 the magnitude of atmospheric inputs is not expected to be very large during early summer.  
316 Further work is required to understand the episodic occurrence of low  $\delta^{15}\text{N}$ -POM.

## 317 **4.2 Biogeochemistry of hypolimnion**

### 318 **4.2.1 Nitrification:**

319 Stratification in the Tillari Reservoir sets in soon after the decline of the monsoon-fed inflow  
320 following which nitrate concentrations increased in oxygenated bottom waters with a  
321 concomitant decrease in ammonium concentrations, indicating the occurrence of nitrification.

322 The nitrate concentrations ranged from below detection limit in the upper 10 m to nearly 10  
323  $\mu\text{M}$  close to the bottom. Nitrification occurs in two steps: ammonia oxidation to nitrite  
324 (performed by ammonia oxidising archaea and bacteria) and nitrite oxidation to nitrate  
325 (performed by nitrite oxidising bacteria). Ammonium, the primary N source, undergoes  
326 strong fractionation producing isotopically light nitrate (Delwiche and Stein, 1970, Casciotti  
327 et al., 2003). The  $\delta^{15}\text{N-NO}_3^-$  values ranged from 2-10‰ and the  $\delta^{18}\text{O-NO}_3^-$  ranged from 5-  
328 8‰ during this period. Nitrate accumulation due to atmospheric deposition and microbial  
329 nitrification will have distinct  $\delta^{18}\text{O-NO}_3^-$  values. This is because, while the oxygen atoms in  
330 atmospheric nitrate are derived from interactions between  $\text{NO}_x$  and  $\text{O}_3$  in the atmosphere,  
331 those in nitrate produced by nitrification come from dissolved oxygen and water ( Kendall,  
332 1998, Finlay et al., 2007). This is well reflected in the  $^{15}\text{N-}^{18}\text{O}$  scatter plot where the  $\delta^{18}\text{O-}$   
333  $\text{NO}_3^-$  data-points from the epilimnion and hypolimnion form completely distinct clusters in  
334 February (Fig 4). As the ammonium pool gets used up, the nitrification rate decreases  
335 accompanied by a decrease in the extent of fractionation (Feigin et al., 1974).

336 Ammonium, oxygen and carbon dioxide are the major substrates needed for nitrification  
337 (Christofi et al., 1981). While ammonium largely comes from the sediments, oxygen is  
338 supplied from aerated surface waters. During the early stratification period, conducive  
339 conditions exist for nitrifiers to grow within the hypolimnion. However, as the bottom waters  
340 turn increasingly more oxygen-depleted with the intensification of stratification the  
341 “ammonium-oxygen chemocline” (Christofi et al., 1981) moves upward in the water column  
342 and the metalimnion becomes more suitable for the occurrence of nitrification. In April 2014,  
343  $\delta^{18}\text{O}$  declined within the thermocline from 34‰ at 5m to 14‰ at 20m owing to nitrification.  
344 Epilimnetic nitrate isotope data are not available for 2012 due to very low nitrate  
345 concentrations. However, the  $\delta^{18}\text{O}$  declined from 25‰ at 15m to 17‰ at 20m. The  $\delta^{15}\text{N}$   
346 values in both the years did not show a similar decline, but this is consistent with the results

347 of several other studies (Böttcher et al., 1990; Burns and Kendall, 2002), where the  $\delta^{18}\text{O}$  was  
348 found to be better suited for source and process identification than  $\delta^{15}\text{N}$ . It may be noted that  
349 this decoupling of  $\delta^{15}\text{N}$  and  $\delta^{18}\text{O}$  was only observed during the peak stratification period at  
350 the thermocline.

351 The  $\delta^{15}\text{N}$  and  $\delta^{13}\text{C}$  values for the POM were generally low during the nitrification period as  
352 also observed in Lake Kinneret (Hadas et al., 2009). The  $\delta^{15}\text{N}$  varied from  $-4\text{‰}$  to  $3\text{‰}$  while  
353  $\delta^{13}\text{C}$  varied from  $-31\text{‰}$  to  $-29\text{‰}$ . Assimilation of newly nitrified  $\text{NO}_3^-$  may be a possible  
354 contributor to POM as indicated by the low  $\delta^{15}\text{N}$  values.

#### 355 **4.2.2 Denitrification:**

356 During the period of strong stratification, the water column loses oxygen below the  
357 thermocline, which apparently results in N loss. Along with a decrease in nitrate, there also  
358 occurs an increase in  $\text{NH}_4^+$  concentration. Dissimilatory nitrate reduction is known to be  
359 associated with 1:1 increase in  $\delta^{15}\text{N-NO}_3^-$  and  $\delta^{18}\text{O-NO}_3^-$  (Granger et al., 2008). Linear  
360 regression of  $\delta^{18}\text{O}$  versus  $\delta^{15}\text{N}$  yielded slope values of 0.95 and 0.85 in 2014 and 2012,  
361 respectively. In canonical denitrification, both  $\delta^{15}\text{N-NO}_3^-$  and  $\delta^{18}\text{O-NO}_3^-$  increase linearly.  
362 The enrichment in isotopic value is  $\sim 1$  in marine systems (Casciotti et al., 2002, Sigman et  
363 al., 2005, Granger et al., 2008). However, this value is reported to be lower (0.5-0.7) in  
364 freshwater systems (Lehmann et al., 2003 and references therein). The reasons for this  
365 difference are not fully understood. Also, studies in freshwater systems are sparse as  
366 compared to marine systems. In a batch of culture experiments, Granger et al. (2008)  
367 observed that nitrate-reducing enzymes play a role in altering the O to N isotopic enrichment,  
368 with periplasmic dissimilatory nitrate reductase (Nap) expressing a lower enrichment value  
369 ( $\sim 0.62$ ) than the membrane-bound dissimilatory nitrate reductase. Again, there is a lack of  
370 data on the isotopic expressions of these enzymes at the ecosystem level. Wenk et al. (2014)

371 attributed the low O:N isotopic effect of  $\sim 0.89$  to chemolithoautotrophic denitrification,  
372 rather than heterotrophic denitrification, in the northern basin of Lake Lugano.

373 Our data from the Tillari reservoir indicates the occurrence of denitrification in the suboxic  
374 hypolimnion under stratified conditions. However, this process is restricted to a narrow depth  
375 range of 10-20 m which limits the number of data points. There may be several factors  
376 responsible for the low ( $< 1$ ) isotopic enrichment factor in the Tillari but our data are not  
377 sufficient to identify the exact cause(s).

378 Assuming the N loss was largely through denitrification, an attempt was made to compute the  
379 fractionation factor using a Rayleigh “closed-system” model (Lehmann et al., 2003).  
380 Although there have been several attempts to compute the nitrogen isotope enrichment  
381 factors in marine systems, ground waters and laboratory cultures (Table 1); similar  
382 information is relatively scarce from freshwater lakes and reservoirs.

383 The available information on oxygen isotope fractionation is even scarcer. The values of  $\epsilon^{15}$   
384 and  $\epsilon^{18}$  computed by us are  $-8.7\text{‰}$  and  $-10.7\text{‰}$ , respectively. The  $\epsilon^{15}$  is much lower than  
385 those obtained from laboratory cultures (Olleros, 1983; Table 1) as well as open-ocean OMZs  
386 (Brandes et al., 1998, Voss et al., 2001; Table 1) although it is close to the  $\epsilon^{15}$  reported from  
387 the eutrophic Lake Lugano. Factors controlling denitrification rates in aquatic systems  
388 include temperature, availability of nitrate and organic carbon, oxygen concentration and type  
389 of bacterium involved (Seitzinger et al., 1988, Bottcher et al., 1990, and references therein).  
390 Sedimentary denitrification is known to incur isotope effect ( $\epsilon^{15}$ ) of  $\sim 0\text{‰}$  due to almost  
391 complete exhaustion of nitrate. The dissolved nitrate concentrations in the Tillari Reservoir  
392 are quite low with the highest values being in the range of 10-12  $\mu\text{M}$  (see Results). The  
393 hypolimnetic nitrate concentrations were even lower ( $< 5 \mu\text{M}$ ) during periods of anoxia. Low  
394 nitrate availability and sedimentary N-loss may exert major controls on the low  $\epsilon^{15}$  observed  
395 in the Tillari Reservoir.



396 Denitrification strongly discriminates among the two N isotopes, leaving behind  $^{15}\text{N}$ -enriched  
397 in the residual  $\text{NO}_3^-$ . POM produced by assimilation of this nitrate will also be enriched in  
398  $^{15}\text{N}$ . However, lower  $\delta^{15}\text{N}$ -PON at these depths implies that  $\text{NH}_4^+$  was the preferred DIN  
399 source. For instance, observations in April 2012 showed that denitrification was active below  
400 30m and associated with ammonium build-up, there was nearly a 4‰ depletion in  $\delta^{15}\text{N}$ -PON  
401 from 2.5‰ (at 30m) to -2.3‰ (at 40m).

#### 402 **4.2.3 Ammonification:**

403 The isotopic composition of ammonium should reflect that of the sedimentary organic matter  
404 being degraded. In Lake Kinneret (Israel),  $\delta^{15}\text{N}$ - $\text{NH}_4^+$  values in the hypolimnion during  
405 stratified conditions ranged from 12 to 17 ‰ reflecting the high  $\delta^{15}\text{N}$  of the sedimentary OM  
406 ( $\delta^{15}\text{N} = 10\text{‰}$ ) (Hadas et al., 2009). In Lake Bled (NW Slovenia), mean  $\delta^{15}\text{N}$ -  $\text{NH}_4^+$  value of  
407 3.8‰ was similar to that of sedimentary OM ( $\delta^{15}\text{N} = 4.5\text{‰}$ ) (Bratkic et al., 2012). Likewise,  
408 the sedimentary OM in the Tillari Reservoir had a  $\delta^{15}\text{N}$  of 2.96‰ similar to the  $\delta^{15}\text{N}$ - $\text{NH}_4^+$   
409 (1.3-2.6‰) thus establishing remineralization of sedimentary OM as the principal  $\text{NH}_4^+$   
410 source.

411 A negative linear relationship between  $\delta^{15}\text{N}$ -PON and  $\ln[\text{NH}_4^+]$  was observed (Fig. 5b) which  
412 further indicated uptake of  $\text{NH}_4^+$ . The fractionation factor ( $\epsilon$ ) calculated from the slope was  
413 -2.4‰. The fractionation factor for ammonium assimilation has been estimated in several  
414 field studies (Cifuentes et al., 1988; Bratkic et al 2012) as well as in lab cultures with  
415 different organisms (green algae, marine bacteria, etc) (Wada & Hattori, 1978, Wada 1980,  
416 Hoch et al 1992). However, such studies in freshwater lakes and reservoirs are scarce. Bratkic  
417 et al. (2012) computed fractionation factors of -0.8‰ and -1.4‰ for mean ammonium  
418 concentrations of 4.7  $\mu\text{M}$  and 3.3  $\mu\text{M}$  respectively in Lake Bled. Hoch et al. (1992) reported  
419 fractionation factor for assimilation by *Vibrio harveyi*, a marine bacterium, to be between

420  $-4\text{‰}$  and  $-27\text{‰}$  for ammonium concentrations ranging from 23 to 180  $\mu\text{M}$ . The fractionation  
421 factor is expected to approach  $0\text{‰}$  for decreased concentrations of ammonium. For the low to  
422 moderate ammonium concentrations recorded (maximum  $\sim 12 \mu\text{M}$  in Figure 5) the  
423 fractionation factor computed by us compares well with previously reported values.

#### 424 **4.2.4 Sulphate reduction and evidence for chemosynthesis:**

425 As the summer intensified and oxidized nitrogen was fully utilized, facultative bacteria  
426 apparently began to utilize sulphate as an electron acceptor as indicated by the accumulation  
427 of  $\text{H}_2\text{S}$ . Mass dependent fractionation during microbial degradation of organic matter with  
428 sulphate as an electron acceptor would the residual organic matter enriched in  $^{13}\text{C}$  and  $^{15}\text{N}$ .  
429 However, following the appearance of  $\text{H}_2\text{S}$ , both  $\delta^{13}\text{C}$ -POC and  $\delta^{15}\text{N}$ -PON became more  
430 depleted. The  $\delta^{15}\text{N}$  values varied between  $-8\text{‰}$  and  $-5\text{‰}$  and  $\delta^{13}\text{C}$  values ranged from  $-37\text{‰}$   
431 to  $-32\text{‰}$  between 30 and 40m depths. The accumulation of  $\text{H}_2\text{S}$  was also accompanied by  
432 significant build-up of  $\text{CH}_4$  (20-150  $\mu\text{M}$ ) and  $\text{NH}_4^+$  (1-20  $\mu\text{M}$ ) (Naik et al., manuscript in  
433 prep.). Increases in POC and PON contents were also observed: from 28  $\mu\text{M}$  to 60  $\mu\text{M}$  for  
434 POC and from 4.7 to 8  $\mu\text{M}$  for PON. Bacterial assimilation of ammonium can explain the  
435 isotopically light nitrogen, but utilization of biogenic methane is known to lead to extremely  
436 low  $\delta^{13}\text{C}$  values (between  $-65\text{‰}$  and  $-50\text{‰}$ ; Whiticar et al., 1986). In our study, the most  
437 depleted  $\delta^{13}\text{C}$ -POC value of  $-37.8\text{‰}$  was associated with the highest methane concentration  
438 of 156  $\mu\text{M}$ . Interestingly, in a study carried out in the waters of Lake Baikal in Siberia, very  
439 negative  $\delta^{13}\text{C}$ -DIC values ( $-28.9$  to  $-35.6\text{‰}$ ) were inferred to be derived from methane  
440 oxidation while the  $\delta^{13}\text{C}$ -POC values ( $-31.7$  to  $-33.5\text{‰}$ ) were typical of lacustrine organic  
441 matter (Prokopenko and Williams 2005). The authors explained this lack of correlation  
442 between the two C pools by a possible time lag between the peak methane oxidation and peak  
443 productivity. Low  $\delta^{13}\text{C}$ -POC ( $\sim -37\text{‰}$ ) in Lake Kinneret was attributed to chemosynthetic C

444 fixation using depleted  $\delta^{13}\text{C}$ -DIC derived from methane oxidation (Hadas et al. 2009). It is  
445 important to understand the fate of methane in freshwater systems as they are believed to be  
446 significant contributors to atmospheric methane emissions (Bastviken et al., 2004). The  
447 POM isotopic data of the Tillari Reservoir provides evidence for intense microbial  
448 chemosynthesis using sulphide, ammonia and methane as energy donors.

#### 449 **4.3 Monsoon mixing in Tillari Reservoir:**

450 The reservoir gets vertically mixed during the months of July, August and September due to a  
451 combination of lower atmospheric temperature, strong winds and inflow of relatively cold  
452 water during the southwest monsoon. Nitrate concentrations are moderately high throughout  
453 the water column, although variable from one year to another. The mean water-column  
454 nitrate concentration were  $7.26\pm 2.8\ \mu\text{M}$  ( $n = 10$ ) in 2011,  $9.29\pm 0.8\ \mu\text{M}$  ( $n = 10$ ) in 2014, and  
455  $8.13\pm 4.7\ \mu\text{M}$  ( $n = 9$ ) in 2015. The isotopic composition of nitrate also showed inter-annual  
456 variability. While the water column was uniformly nitrate-replete in 2014, the epilimnetic (0-  
457 5 m) nitrate concentrations in 2011 and 2015 were markedly lower than those at deeper  
458 depths (Fig.7), except at two deepest samples in 2015. This may indicate nitrate uptake by  
459 phytoplankton. However, considering its high concentration in rainwater, ammonium is  
460 expected to compete with nitrate for phytoplankton uptake. Moreover, the  $\delta^{15}\text{N}$  of nitrate in  
461 the epilimnion was lower in 2011 and 2015 than in 2014. In fact, elevated values of  $\delta^{15}\text{N}$ -  
462  $\text{NO}_3^-$  ( $>8\text{‰}$ ) occurred throughout the water column in 2014 when the nitrate concentration  
463 was also generally higher as compared to the other two years. To investigate the cause of this  
464 variability, water samples from six upstream stations along the Tillari River along with a  
465 rainwater sample at the main station were collected in 2015. The nitrate concentrations  
466 ranged from  $1.8\ \mu\text{M}$  at the most upstream station to  $9.4\ \mu\text{M}$  close to our main sampling site.  
467 The ranges of  $\delta^{15}\text{N}$  and  $\delta^{18}\text{O}$  of  $\text{NO}_3^-$  at these stations were 0.4-6.8‰ and 11-27‰,

468 respectively. The rainwater sample had a nitrate content of 13.89  $\mu\text{M}$  (ammonium = 24.4  
469  $\mu\text{M}$ ) and yielded  $\delta^{15}\text{N}$  and  $\delta^{18}\text{O}$  values of  $-2.9\text{‰}$  and  $88.7\text{‰}$ , respectively. Nitrate in wet  
470 deposition is usually characterised by high  $\delta^{18}\text{O}$  ( $> 60\text{‰}$ ) (Kendall et al., 2007; Thibodeau et  
471 al., 2013) and low  $\delta^{15}\text{N}$  ( $-10$  to  $+5 \text{‰}$ ) (Heaton et al., 2004) values. Unfortunately, the  
472 concentration and isotopic composition of these end members (river runoff and atmospheric  
473 deposition) do not explain the data from the Tillari especially from the 2015. Based on the  
474 high concentration of nitrate in rainwater, it is tempting to suggest that it could be an  
475 important source, but the isotopic data show a mismatch. The  $\delta^{13}\text{C}$ -POC values in the  
476 epilimnion decreased to nearly  $-30\text{‰}$  presumably due to a combination of lower primary  
477 productivity and inputs of organic matter through runoff. Even though the latter was not  
478 measured POC derived from land vegetation is expected to be isotopically light. The POM  
479 data show the ingress of a nearly 30m thick parcel of water from the Tillari River into the  
480 reservoir. This ingress is apparent below 5m depth by distinct  $\delta^{13}\text{C}$  and  $\delta^{15}\text{N}$  of POM. The  
481  $\delta^{13}\text{C}$ -POC increases from  $-30.9\text{‰}$  ( $\pm 0.1\text{‰}$ ) in the upper 5m to  $-25.4\text{‰}$  ( $\pm 1\text{‰}$ ) between 5m  
482 and 40m. Below 40m, the mean  $\delta^{13}\text{C}$ -POC was  $-26.5\text{‰}$  ( $\pm 1.7\text{‰}$ ). The mean  $\delta^{15}\text{N}$  of the  
483 intermediate water parcel was  $5.97 \pm 2\text{‰}$ , as compared to  $5.49 \pm 3\text{‰}$  in the bottom waters and  
484  $3.96 \pm 2\text{‰}$  in the upper 5m. The isotopic data correspond well with the ancillary chemical  
485 parameters, in that the water parcel had a distinct thermal signature (cooler by nearly  $2^\circ\text{C}$ ). It  
486 also possessed higher levels of nitrate and lower levels of DO and chlorophyll-*a*.

487 Thus, looking solely at the high nitrate concentrations in the water column, atmospheric wet  
488 deposition may be a major nitrate source to the water column during the monsoon season.  
489 However, this inference is based on a single measurement where the isotopic composition is  
490 also different. Moreover, the river water is also rain-fed and it is not clear why its isotopic  
491 composition is much lower at the most upstream station. At the same time, the isotopic  
492 composition of POM indicates influence of the upstream waters. Variable inputs from the

493 atmosphere and by river runoff to the DIN pool probably account for the interannual  
494 variability, but more studies are needed to identify and quantify these contributions in detail.

## 495 **5. Summary and Conclusions:**

496 Using stable isotopes of nitrate, ammonium and particulate organic matter, we have been able  
497 to identify distinct water column conditions and transformation processes of reactive nitrogen  
498 in the Tillari Reservoir. The reservoir gets vertically mixed during the southwest monsoon  
499 season as well as in winter; the water column remained stratified during other parts of the  
500 year. The most intense stratification occurs during summer just before the monsoon onset.  
501 Relative importance of microbial processes such as nitrification, denitrification,  
502 ammonification and sulphate reduction in the water column varied depending on intensity of  
503 stratification and associated DO levels in the hypolimnion. These processes produced unique  
504 isotopic signatures in the dissolved and particulate matter. Our results suggest the occurrence  
505 of microbial chemosynthesis using methane and ammonium as primary C- and N- sources,  
506 producing organic matter in the anoxic bottom waters that is highly depleted in  $^{13}\text{C}$  and  $^{15}\text{N}$   
507 content. The thermocline in the Tillari Reservoir has been known to harbour photoautotrophic  
508 sulphur bacteria during peak stratification periods (Kurian et al., 2012). We also found strong  
509 signatures of nitrification within this zone during summer stratification. Autochthonous  
510 production was the principal source of organic matter in the epilimnion which was well-  
511 oxygenated at all times, although productivity was significantly lower during the monsoon  
512 period due to light-limited conditions. Nitrate was the preferred DIN source in the  
513 epilimnion. When nitrate loss occurred in the hypolimnion, the preferred DIN species  
514 switched from nitrate to ammonium. Isotopic measurement of precipitation and upstream  
515 river samples during one seasonal sampling provided some insight into sources of nitrogen,  
516 but the observed inter-annual variability could not be explained. Overall, solar intensity,

517 water depth and redox conditions appear to be the major factors controlling biogeochemical  
518 cycling in this pristine reservoir.

### 519 **Acknowledgements:**

520 We thank the Director, CSIR-NIO for providing necessary support for this work and the  
521 management body of the Tillari reservoir for permission to carry out this study. This research  
522 was carried out as a part of INDIAS IDEA project funded by the Council of Scientific &  
523 Industrial Research (CSIR). The authors wish to thank Mark Altabet and Laura Bristow for  
524 sharing their expertise. We thank Prof. Sugata Hazra and the School of Oceanographic  
525 Studies, Jadavpur University for their support and encouragement. Puja Satardekar is  
526 acknowledged for analyzing the nutrient samples. Sujal Bandodkar (DTP section, CSIR-NIO)  
527 is thanked for her creative inputs. P. Bardhan thanks CSIR for the award of Senior Research  
528 Fellowship. The authors are also grateful to Ms. Maya MV for her initial assistance in  
529 isotopic analyses and to Mr. H. Dalvi, Mr. A. Methar, Mr. Jonathan and Mr. Sumant for their  
530 help during field work. This is NIO Contribution no. XXXX.

### 531 **References**

- 532 Altabet, M. A.: Variations in nitrogen isotopic composition between sinking and suspended  
533 particles: Implications for nitrogen cycling and particle transformation in the open ocean,  
534 *Deep-Sea Res.*, 35, 535–554, 1988.
- 535  
536 Altabet, M. A.: Isotopic tracers of the marine nitrogen cycle, in: *Marine organic matter:  
537 Chemical and biological markers*, edited by: Volkman, J., *The handbook of environmental  
538 chemistry*, Springer-Verlag, 251–293, 2006.
- 539  
540 Bastviken, D., Cole, J. J., Pace, M., and Tranvik, L.: Methane emissions from lakes:  
541 Dependence of lake characteristics, two regional assessments, and a global estimate, *Glob.  
542 Biogeochem. Cy.*, 18:GB4009, doi: 10.1029/2004GB002238, 2004.
- 543  
544 Böttcher, J., Strebel, O., Voerkelius, S., and Schmidt, H.-L.: Using isotope fractionation of  
545 nitrate-nitrogen and nitrate-oxygen for evaluation of microbial denitrification in a sandy  
546 aquifer, *J. Hydrol.*, 114, 413–424, doi: 10.1016/0022-1694(90)90068-9, 1990.
- 547  
548 Brandes, J. A., Devol, A. H., Yoshinari, T., Jayakumar, D. A., and Naqvi, S. W. A.: Isotopic  
549 composition of nitrate in the central Arabian Sea and eastern tropical North Pacific: A tracer

550 for mixing and nitrogen cycles, *Limnol. Oceanogr.*, 43, 1680–1689, doi:  
551 10.4319/lo.1998.43.7.1680, 1998.

552

553 Bratkic, A., Sturm, M., Faganeli, J., and Ogrinc, N.: Semi-annual carbon and nitrogen isotope  
554 variations in the water column of Lake Bled, NW Slovenia, *Biogeosciences*, 9, 1–11. doi:  
555 10.5194/bg-9-1-2012, 2012.

556

557 Burns, D. A. and Kendall, C.: Analysis of  $^{15}\text{N}$  and  $^{18}\text{O}$  sources in runoff at two watersheds in  
558 the Catskill Mountains of New York, *Water Resour. Res.*, 38, 1051, doi: 10.1029/  
559 2001WR000292, 2002.

560

561 Carpenter, E. J., Harvey, H. R., Fry, B., and Capone, D. G.: Biogeochemical tracers of the  
562 marine cyanobacterium *Trichodesmium*, *Deep-Sea Res. Pt. I*, 44, 27–38, 1997.

563

564 Casciotti, K. L., Sigman, D. M., Galanter Hastings, M., Bohlke, J. K., and Hilkert, A.:  
565 Measurement of the oxygen isotopic composition of nitrate in seawater and freshwater using  
566 the denitrifier method, *Anal. Chem.*, 74, 4905–4912, 2002.

567 Casciotti, K. L., Sigman, D. M., and Ward, B. B.: Linking diversity and stable isotope  
568 fractionation in ammonia-oxidizing bacteria, *Geomicrobiol. J.*, 20, 335–353, 2003.

569

570 Chen, F. J. and Jia, G. D.: Spatial and seasonal variations in  $\delta^{13}\text{C}$  and  $\delta^{15}\text{N}$  of particulate  
571 organic matter in a dam-controlled subtropical river, *River Res. Appl.*, 25, 1169–1176, doi:  
572 10.1002/rra.1225, 2009.

573

574 Chen, F., Jia, G., and Chen, J.: Nitrate sources and watershed denitrification inferred from  
575 dual isotopes in the Beijiang River, South China, *Biogeochemistry*, 94, 163–174, doi:  
576 10.1007/s10533-009-9316-x, 2009.

577

578 Chen, Z.X., Yu, L., Liu, W.G., Lam, M.H.W., Liu, G.J., and Yin, X. B.: Nitrogen and oxygen  
579 isotopic compositions of water-soluble nitrate in Taihu Lake water system, China:  
580 implication for nitrate sources and biogeochemical process, *Environ Earth Sci.*, 1, 217–223,  
581 2014.

582

583 Christofi, N., Preston, T. and Stewart, W.D.P.: Endogenous nitrate production in an  
584 experimental enclosure during summer stratification, *Water research*, 15(3), 343-349, doi:  
585 10.1016/0043-1354(81)90039-7, 1981.

586

587 Cifuentes, L. A., Sharp, J. H., and Fogel, M. L.: Stable carbon and nitrogen isotope  
588 biogeochemistry in the Delaware Estuary, *Limnol. Oceanogr.*, 33, 1102–1115, 1988.

589

590 Cline, J.D.: Spectrophotometric determination of hydrogen sulfide in natural waters, *Limnol.*  
591 *Oceanogr.*, 14, 454–458, 1969.

592

593 Dähnke, K., and Thamdrup, B.: Nitrogen isotope dynamics and fractionation during  
594 sedimentary denitrification in Boknis Eck, Baltic Sea, *Biogeosciences*, 10, 3079–3088. doi:  
595 10.5194/bg-10-3079-2013, 2013.

596

597 Delwiche, C. C., and Stein, P. L.: Nitrogen isotope fractionation in soil and microbial  
598 reactions, *Environ. Sci. Tech.*, 4, 929-935, 1970.

599

600 Feigin, A., Shearer, G., Kohl, D. H. and Comner, B.: The amount and nitrogen-15 content  
601 of nitrate in soil profiles from two central Illinois fields in a corn-soybean rotation, *Soil Sci.*  
602 *Soc. Amer. Proc.*, 38, 465–471, 1974.

603

604 Finlay, J. C., Sterner, R. W., and Kumar, S.: Isotopic evidence for in-lake production of  
605 accumulating nitrate in Lake Superior, *Ecol. Appl.*, 17, 2323–2332, doi: 10.1890/07-0245.1,  
606 2007.

607

608 Granger, J., Sigman, D. M., Lehmann, M. F., and Tortell, P. D.: Nitrogen and oxygen isotope  
609 fractionation during dissimilatory nitrate reduction by denitrifying bacteria, *Limnol.*  
610 *Oceanogr.*, 53, 2533–2545, 2008.

611

612 Grasshoff, K., Ehrhardt, M., and Kremling, K.: *Methods of seawater analysis*, 2 Edn., 419  
613 pp., Weinheim: Verlag Chemie., 1983.

614 Gu, B., Chapman, A. D., and Schelske, C. L.: Factors controlling seasonal variations in stable  
615 isotope composition of particulate organic matter in a soft water eutrophic lake, *Limnol.*  
616 *Oceanogr.*, 51, 2837–2848, 2006.

617

618 Hadas, O., Altabet, M. A., and Agnihitori, R.: Seasonally varying nitrogen isotope  
619 biogeochemistry of particulate organic matter in lake Kinneret, Israel, *Limnol. Oceanogr.*, 54,  
620 75–85, 2009.

621

622 Heaton, T. H. E.: Isotopic studies of nitrogen pollution in the hydrosphere and atmosphere: A  
623 review, *Chem. Geol.*, 59, 87–102, 1986.

624

625 Hoch, M. P., Fogel, M. L., and Kirchner, D. L.: Isotope fractionation associated with  
626 ammonium uptake by a marine bacterium, *Limnol. Oceanogr.*, 37, 1447–1459, 1992.

627

628 Holmes, R. M., McClelland, J. W., Sigman, D. M., Fry, B., and Peterson, B. J.: Measuring  
629  $^{15}\text{N-NH}_4^+$  in marine, estuarine and fresh waters: an adaptation of the ammonia diffusion  
630 method for samples with low ammonium concentrations, *Mar. Chem.*, 60, 235–243,  
631 doi: 10.1016/S0304-4203(97)00099-6, 1998.

632

633 Hu, H., Bourbonnais, A., Larkum, J., Bange, H. W., and Altabet, M. A.: Nitrogen cycling in  
634 shallow low oxygen coastal waters off Peru from nitrite and nitrate nitrogen and oxygen  
635 isotopes. *Biogeosciences Discussions* 12, 7257–7299, doi: 10.5194/bgd-12-7257-2015, 2015.

636

637 Junet, A. de, Abril, G., Gu'erin, F., Billy, I., and Wit, R. de.: A multi-tracers analysis of  
638 sources and transfers of particulate organic matter in a tropical reservoir (Petit Saut, French  
639 Guiana), *River Res. Appl.*, 25, 253–271, doi:10.1002/rra.1152, 2009.

640

641 Kendall, C.: Tracing nitrogen sources and cycling in catchments, in: *Isotope tracers in*  
642 *catchment hydrology*, edited by: Kendall, C. and McDonnell, J.J., Elsevier, Amsterdam, The  
643 Netherlands, 519–576, 1998.

644

645 Kendall, C., Silva, S. R., and Kelly, V. J.: Carbon and nitrogen isotopic compositions of  
646 particulate organic matter in four large river systems across the United States, *Hydrol.*  
*Process.*, 15, 1301–1346, doi: 10.1002/hyp.216, 2001



647 Kendall, C., Elliott, E. M., and Wankel, S. D.: Tracing anthropogenic inputs of nitrogen to  
648 ecosystems, Chapter 12, in: *Stable Isotopes in Ecology and Environmental Science*, edited  
649 by: Michener, R. H. and Lajtha, K., 2nd Edition, Blackwell Publishing, 375–449, 2007.  
650

651 Kritee, K., Sigman, D.M., Granger, J., Ward, B.B., Jayakumar, A., and Deutsch, C.: Reduced  
652 isotope fractionation by denitrification under conditions relevant to the ocean, *Geochim.*  
653 *Cosmochim. Acta*, 92, 243–259, doi:10.1016/j.gca.2012.05.020, 2012.  
654

655 Kurian, S., Roy, R., Repeta, D.J., Gauns, M., Shenoy, D.M., Suresh, T., Sarkar, A.,  
656 Narvenkar, G., Johnson, C.G., and Naqvi, S.W.A.: Seasonal occurrence of anoxygenic  
657 photosynthesis in Tillari and Selaulim reservoirs, Western India, *Biogeosciences*, 9, 2485–  
658 2495, doi:10.5194/bg-9-2485-2012, 2012.  
659

660 Lehmann, M. F., Reichert, P., Bernasconi, S. M., Barbieri, A., and McKenzie, J.: Modelling  
661 nitrogen and oxygen isotope fractionation during denitrification in a lacustrine redox-  
662 transition zone, *Geochim. Cosmochim. Ac.*, 67, 2529–2542, doi: 10.1016/S0016-  
663 7037(03)00085-1, 2003  
664

665 Lehmann, M. F., Bernasconi, S., McKenzie, J., Barbieri, A., Simona, M., and Veronesi, M.:  
666 Seasonal variation of the  $\delta^{13}\text{C}$  and  $\delta^{15}\text{N}$  of particulate and dissolved carbon and nitrogen in  
667 Lake Lugano: Constraints on biogeochemical cycling in a eutrophic lake, *Limnol. Oceanogr.*,  
668 49, 415–429, 2004.  
669

670 Maya, M. V., Karapurkar, S. G., Naik, H., Roy, R., Shenoy, D. M., and Naqvi, S. W. A.:  
671 Intra-annual variability of carbon and nitrogen stable isotopes in suspended organic matter in  
672 waters of the western continental shelf of India, *Biogeosciences*, 8, 3441– 3456,  
673 doi:10.5194/bg-8-3441-2011, 2011.  
674

675 McIlvin, M. R. and Altabet, M. A.: Chemical conversion of nitrate and nitrite to nitrous oxide  
676 for nitrogen and oxygen isotopic analysis in freshwater and seawater, *Anal. Chem.*, 77, 5589–  
677 5595, doi: 10.1021/ac050528s, 2005.  
678

679 Mengis, M., Schiff, S. L., Harris, M., English, M. C., Aravena, R., Elgood, R. J., and  
680 MacLean, A.: Multiple geochemical and isotopic approaches for assessing ground water  
681  $\text{NO}_3^-$  elimination in a riparian zone, *Ground Water*, 37, 448–457, 1999.  
682

683 Narvenkar, G., Naqvi, S. W. A., Kurian, S., Shenoy, D. M., Pratihary, A. K., Naik, H., Patil,  
684 S., Sarkar, A., and Gauns, M.: Dissolved methane in Indian freshwater reservoirs, *Environ*  
685 *Monit Assess*, 185(8), 6989–6999, 2013.  
686

687 Olleros, T.: Kinetische Isotopeneffekte der Arginase- und Nitratreduktase-Reaktion: Ein  
688 Beitrag zur Aufklärung der entsprechenden Reaktionsmechanismen, Ph.D. dissertation,  
689 Technische Universität München-Weihenstephan, Germany, 1983.  
690

691 Pang, P. C., and Nriagu, J. O.: Isotopic variations of the nitrogen in Lake Superior, *Geochim.*  
692 *Cosmochim. Acta*, 41, 811–814, doi: 10.1016/0016-7037(77)90051-5, 1977.  
693

694 Prokopenko, A. A., and Williams, D.F.: Depleted methane-derived carbon in waters of Lake  
695 Baikal, Siberia, *Hydrobiol.*, 544, 279–288, 2005.  
696

697 Savoye, N., David, V., Morisseau, F., Etcheber, H., Abril, G., Billy, I., Charlier, K., Oggian,  
698 G., Derriennic, H., and Sautour, B.: Origin and composition of particulate organic matter in a  
699 macrotidal turbid estuary: the Gironde Estuary, France, *Estuar. Coast. Shelf Sci.*, 108, 16-28,  
700 doi: 10.1016/j.ecss.2011.12.005, 2012.

701 Seitzinger, S. P.: Denitrification in freshwater and coastal marine ecosystems: Ecological and  
702 Geochemical significance, *Limnol. Oceanogr.*, 33, 702–724, 1988.

703

704 Sigman, D. M., Robinson, R., Knapp, A. N., Van Geen, A., McCorkle, D. C., Brandes, J. A.,  
705 and Thunell, R. C.: Distinguishing between water column and sedimentary denitrification in  
706 the Santa Barbara Basin using the stable isotopes of nitrate. *Geochem. Geophys. Geosy.*, 4,  
707 1040, doi:10.1029/2002GC000384, 2003.

708

709 Sigman, D. M., Granger, J., DiFiore, P. J., Lehmann, M. M., Ho, R., Cane, G., and van Geen,  
710 A.: Coupled nitrogen and oxygen isotope measurements of nitrate along the eastern North  
711 Pacific margin, *Global Biogeochem. Cy.*, 19, GB4022, doi:10.1029/2005GB002458, 2005.

712

713 Subramanya, K.: *Engineering Hydrology*, 4<sup>th</sup> edition, McGraw-Hill Publishing, New Delhi,  
714 2013.

715

716 Sukumar, R., Suresh, H. S., and Ramesh, R.: Climate change and its impact on tropical  
717 montane ecosystems in southern India. *J. Biogeogr.*, 22, 533-536, 1995.

718

719 Thibodeau, B., Hélie, J.-F., and Lehmann, M. F.: Variations of the nitrate isotopic  
720 composition in the St. Lawrence River caused by seasonal changes in atmospheric nitrogen  
721 inputs, *Biogeochemistry*, 115, 287–298, 2013.

722

723 Thunell, R. C., Sigman, D. M., Muller-Karger, F., Astor, Y., and Varela, R.: Nitrogen isotope  
724 dynamics of the Cariaco Basin, Venezuela, *Global Biogeochem. Cy.*, 18, GB3001,  
725 doi:10.1029/2003GB002185, 2004.

726

727 Voss, M., Dippner, J. W., and Montoya, J. P.: Nitrogen isotope patterns in the oxygen-  
728 deficient waters of the Eastern Tropical North Pacific Ocean, *Deep-Sea Res. Pt. 1*, 48, 1905–  
729 1921, doi:10.1016/S0967-0637(00)00110-2, 2001.

730

731 Wada, E. and Hattori, A.: Nitrogen isotope effects in the assimilation of inorganic  
732 compounds by marine diatoms, *Geomicrobiol. J.*, 1, 85–101, 1978.

733

734 Wada, E.: Nitrogen isotope fractionation and its significance in biogeochemical processes  
735 occurring in marine environments, in: *Isotope Marine Chemistry*, edited by: Goldberg, E. D.,  
736 Horibe, Y., and Saruhashi, K., Uchida Rokakuho Pub. Co., Tokyo, 375–398, 1980.

737

738 Wankel, S. D., Kendall, C., Pennington, J. T., Chavez, F. P., and Paytan, A.: Nitrification in  
739 the euphotic zone as evidenced by nitrate dual isotopic composition: Observations from  
740 Monterey Bay, California, *Global Biogeochem. Cy.*, 21, GB2009,  
741 doi:10.1029/2006gb002723, 2007.

742

743 Wenk, C. B., Zopfi, J., Brees, J., Veronesi, M., Niemann, H., and Lehmann, M. F.:  
744 Community N and O isotope fractionation by sulfide-dependent denitrification and anammox  
745 in a stratified lacustrine water column, *Geochim. Cosmochim. Acta*, 125, 551-563, 2014.

746 Whiticar, M. J., Faber, E., and Schoell, M.: Biogenic methane formation in marine and  
747 freshwater environments:CO<sub>2</sub> reduction vs. acetate fermentation-isotope evidence, *Geochim*  
748 *Cosmochim Acta*, 50, 693-709, 1986.

749  
750  
751  
752  
753  
754  
755  
756  
757  
758  
759  
760

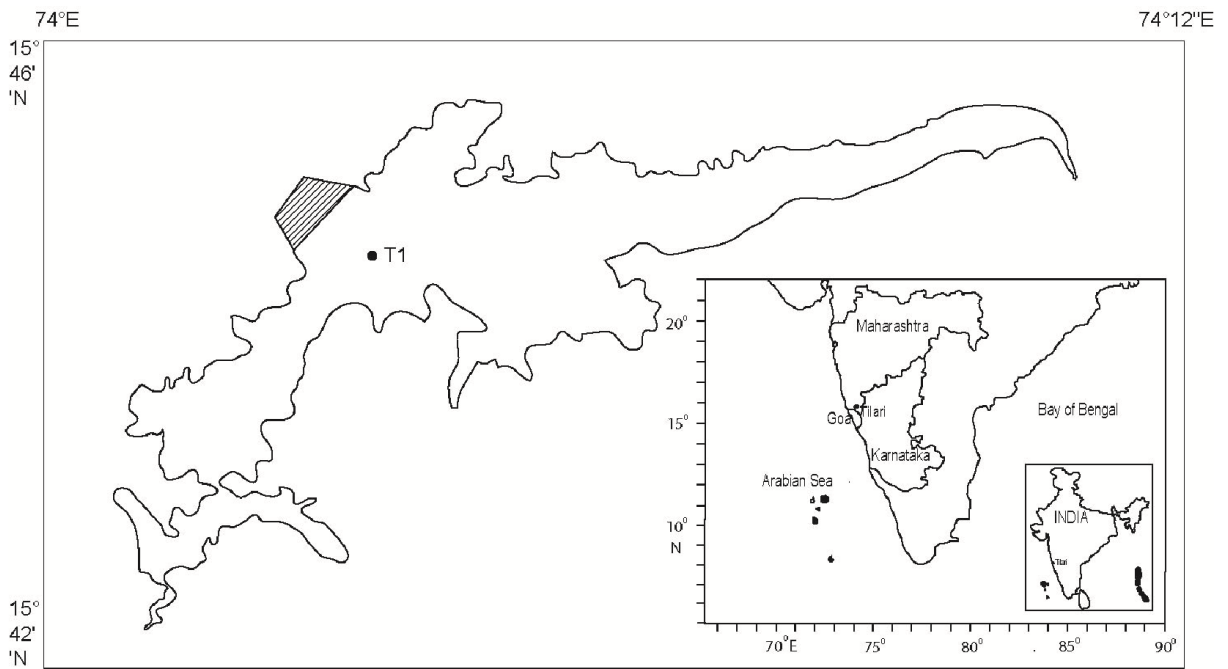
761 Table 1: The values of nitrogen ( $\epsilon^{15}$ ) and oxygen ( $\epsilon^{18}$ ) isotope effects for denitrification as  
 762 reported from some natural systems as well as laboratory cultures.

763  
 764

Study Area	$\epsilon^{15}$ (‰)	$\epsilon^{18}$ (‰)	Reference
Cariaco Basin, Venezuela	-1.5		<i>Thunell et al., 2004</i>
Beijiang River, China	-14.8	-8.5	<i>Chen et al., 2009</i>
Boknis Eck, Baltic Sea	-18.9	-15.8	<i>Dahnke and Thamdrup, 2013</i>
Lake Lugano, Switzerland	-11.2	-6.6	<i>Lehmann et al., 2003</i>
Groundwater	-27.6	-18.3	<i>Mengis et al., 1999</i>
Denitrifier culture	-30	-15	<i>Olleros, 1983</i>
Denitrifier culture	-10 to -15		<i>Kritee et al., 2012</i>
Open-ocean OMZs	-20 to -30		<i>Brandes et al., 1998; Voss et al., 2001</i>
Shallow groundwater aquifer	-15.9	-8	<i>Bottcher et al., 1990</i>
Tillari reservoir, India	-8.73	-10.74	<b>This study</b>

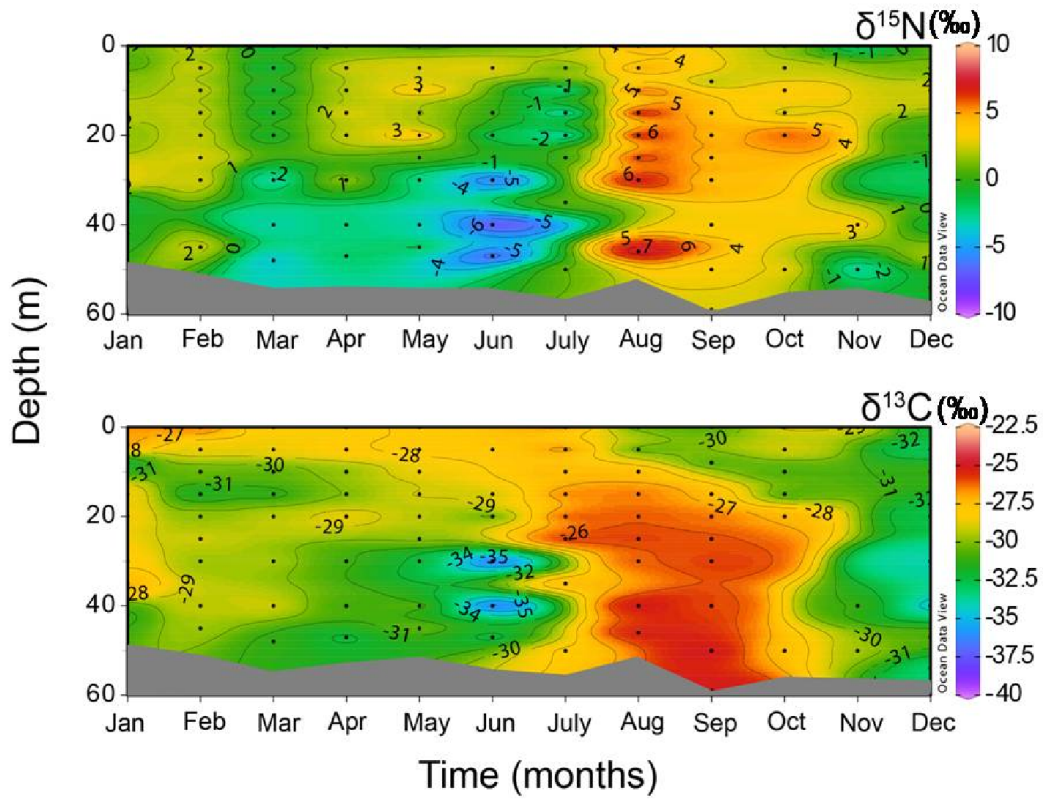
765  
 766  
 767  
 768  
 769  
 770  
 771  
 772  
 773  
 774  
 775  
 776  
 777  
 778  
 779  
 780  
 781  
 782  
 783  
 784

785 **Figure 1: Map of the sampling location (Tillari Reservoir). T1 shows the main sampling**  
786 **location at the deepest point of the reservoir.**



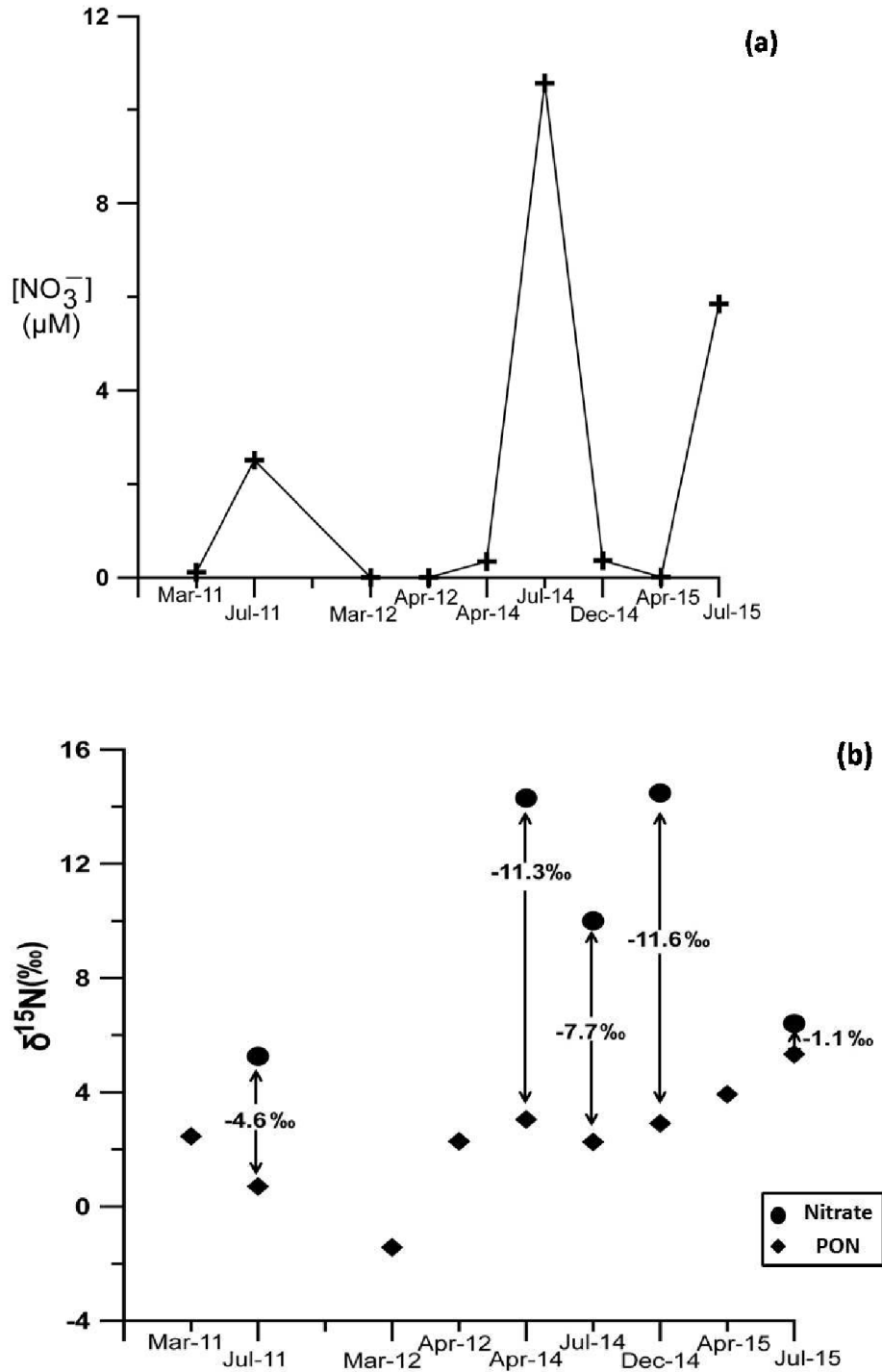
787  
788  
789  
790  
791  
792  
793  
794  
795  
796  
797  
798  
799  
800  
801

802 **Figure 2: Mean annual variations of  $\delta^{15}\text{N-POM}$  and  $\delta^{13}\text{C-POM}$  at the main sampling**  
803 **location.**



804  
805  
806  
807  
808  
809  
810  
811  
812  
813  
814  
815  
816

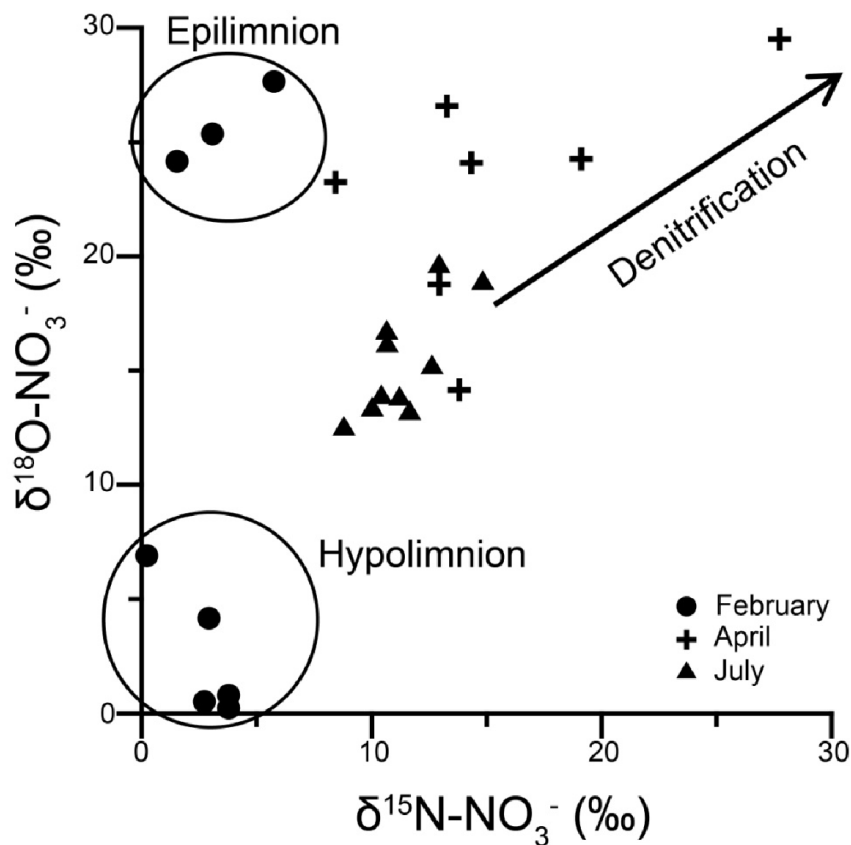
817 **Figure 3: Time-series of nitrate concentrations (a) and  $\delta^{15}\text{N}$  of dissolved nitrate and**  
 818 **POM in the epilimnion (0-5 m) (b). The isotopic differences between the dissolved and**  
 819 **particulate species have been denoted by arrows. Each data point represents one**  
 820 **sample. Each data point represents a single sample.**



821

822

823 **Figure 4: Nitrogen and oxygen isotopic composition of dissolved nitrate during three**  
 824 **different periods in 2014. February represents the early or weak stratification period**  
 825 **with two distinct clusters of epilimnetic (0-10 m) and hypolimnetic (15-48 m) samples.**  
 826 **April is a period of intense water-column stratification and denitrification signal is**  
 827 **observed in the bottom waters. July is a period of monsoon holomixis when the water**  
 828 **column has uniformly high nitrate values.**

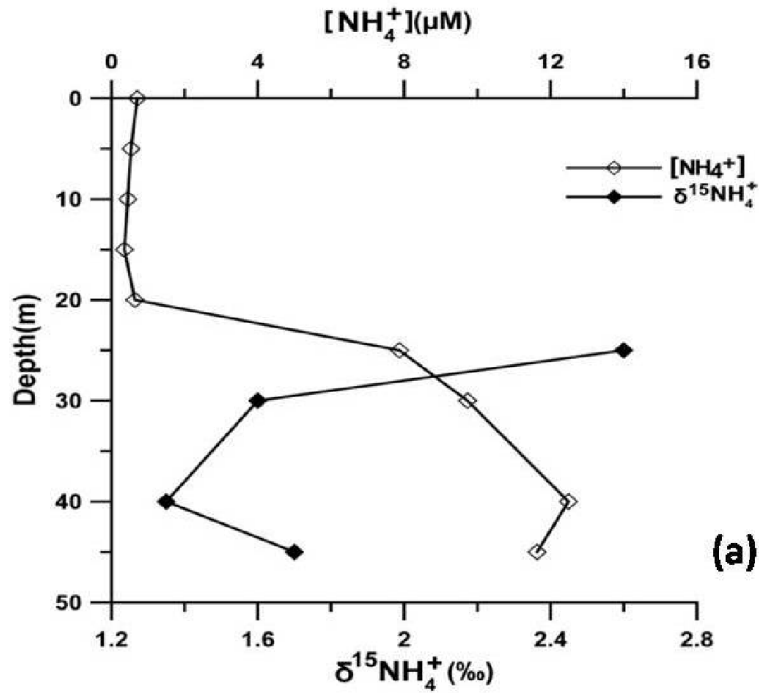


829  
 830  
 831  
 832  
 833  
 834  
 835

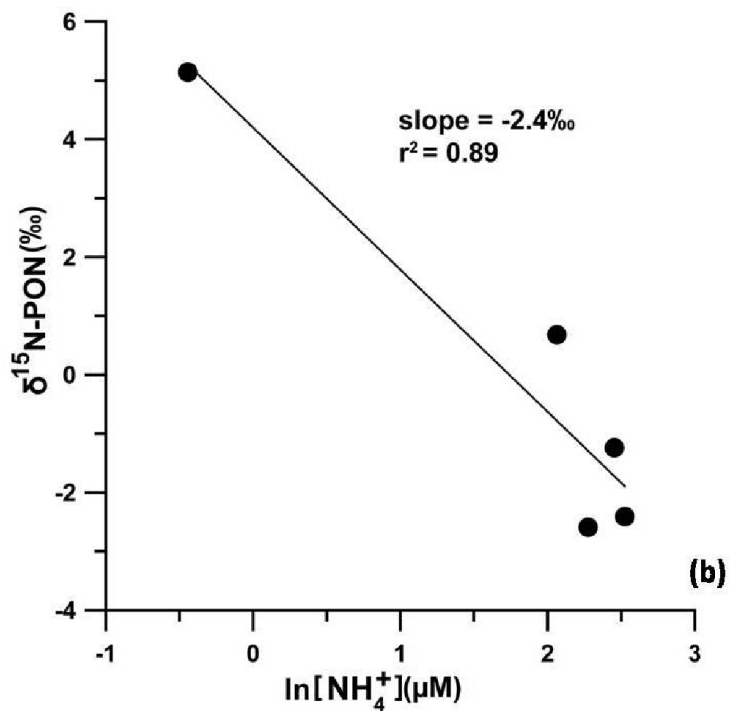


836 **Figure 5: (a) Depth-wise variations of ammonium concentration and  $\delta^{15}\text{N-NH}_4^+$  in May**  
 837 **2012. (b) Plot of  $\delta^{15}\text{N-PON}$  versus  $\ln(\text{NH}_4^+)$ . The negative linear correlation yields a**  
 838 **fractionation factor ( $\epsilon$ ) of -2.4‰. Each data point represents a single sample.**

839

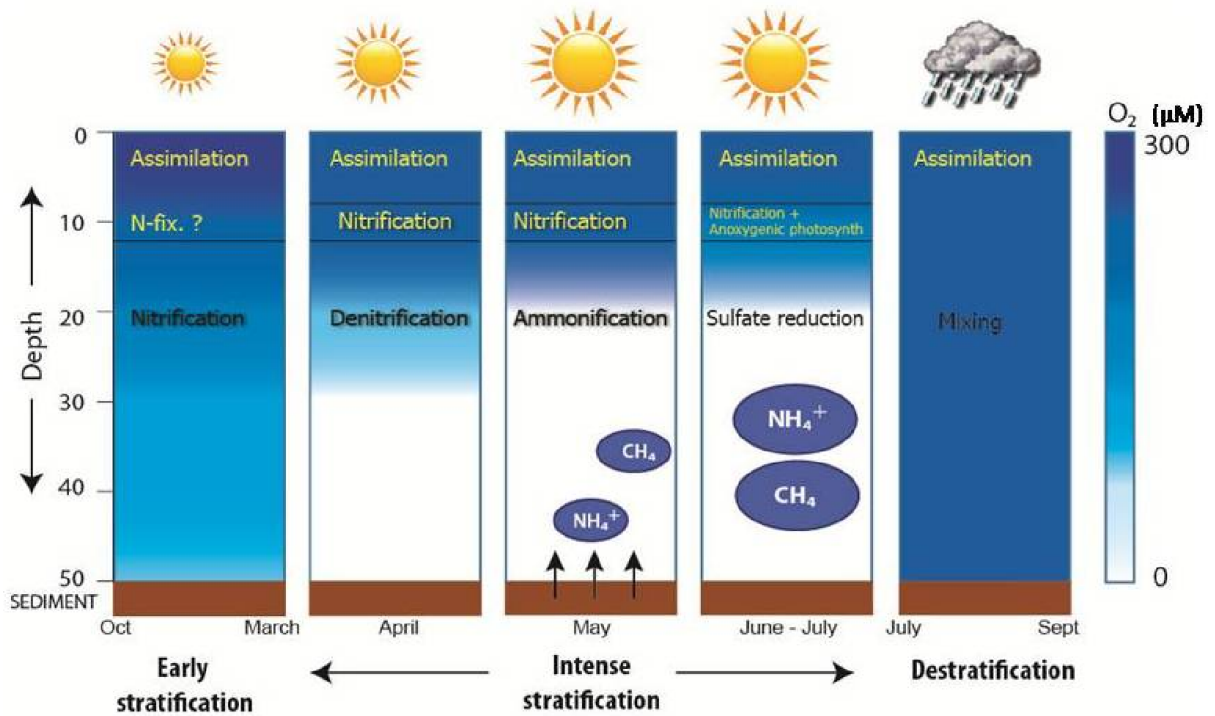


840



841

842 **Figure 6: Schematic diagram depicting major biogeochemical processes taking place in**  
 843 **the Tillari Reservoir over an annual cycle. This information is based on monthly**  
 844 **sampling in the reservoir for several years (Shenoy et al., manuscript in preparation)**



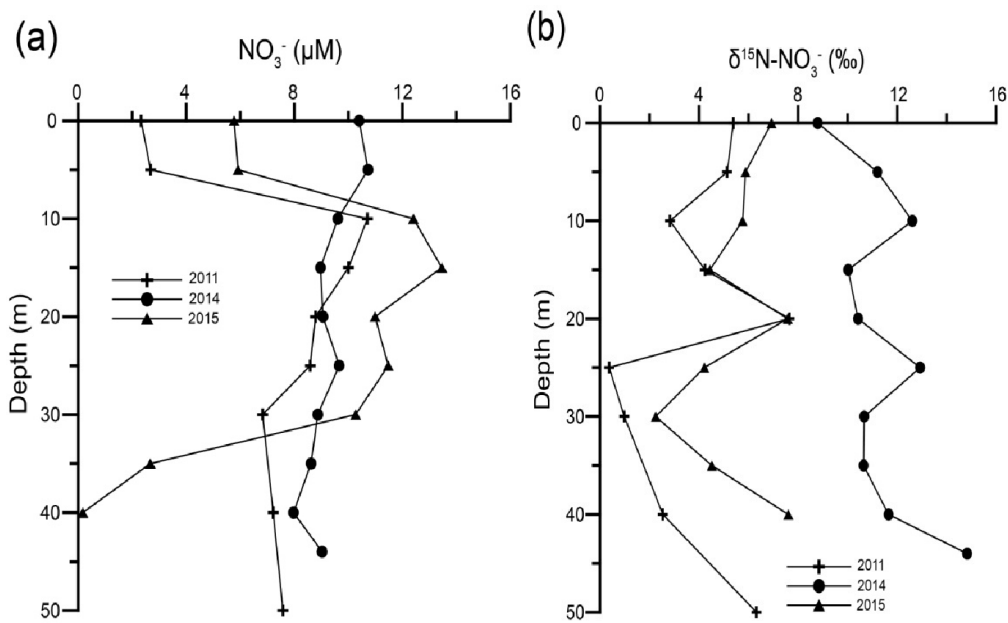
845  
 846  
 847  
 848  
 849  
 850  
 851  
 852  
 853  
 854  
 855  
 856

857 **Figure 7: Vertical profiles of  $\text{NO}_3^-$  (a) and  $\delta^{15}\text{N-NO}_3^-$  (b) during monsoon mixing in**  
858 **2011, 2014 and 2015. Each profile is from one field trip during the peak SWM in a given**  
859 **year with each data point representing one sample.**

860

861

862



863